Quantum Electronics **41** (3) 239 – 242 (2011)

LASER RESONATORS

PACS numbers: 42.60.Da; 42.60.Jf; 07.60.Ly
DOI: 10.1070/QE2011v041n03ABEH014410

Mirror with a variable amplitude – phase reflectance. 2. Modelling of a laser resonator with an active output mirror

V.V. Kiiko, V.I. Kislov, E.N. Ofitserov

***Abstract*. We present the operator model of the laser resonator with an active output mirror based on the Fabry – Perot interferometer with nonflat (spherical and aspherical) mirrors and an adjustable gap. The results of numerical simulation of a microchip laser with a thermal lens and an active output interferometer-based mirror are given. It is shown that the use of an active interferometer as the output cavity mirror allows one to control the number of transverse modes of laser radiation and its power; in this case, the beam divergence can be reduced by a factor of 1.5 – 2.5.**

Keywords: *laser resonator with an active output mirror, radiation divergence and transverse modes.*

1. Introduction

The design and development of microchip lasers is one of the promising directions of laser technology [1, 2]. The potential of the control of the spatiotemporal radiation characteristics of microchip lasers is limited. Thus, the time characteristics of radiation (repetition rate, pulse duration) of a passively Q-switched, high-frequency microchip laser can be controlled by varying the pump power. In this case, the thermal lens power in the active element [3] and spatiotemporal characteristics of the output radiation change; the divergence of output radiation increases [4].

One way to control the output parameters of microchip lasers is based on the use of an active mirror with controlled reflectivity based the Fabry – Perot interferometer as the output mirror [5 – 7]. However, the authors of these papers did not consider the potential of a system consisting of a laser resonator and an interferometer-based mirror. In this work we have investigated the effect of the active mirror on the mode composition, power, and divergence of output radiation of a microchip laser.

V.V. Kiiko, V.I. Kislov, E.N. Ofitserov A.M. Prokhorov General Physics Institute, Russian Academy of Sciences, ul. Vavilova 38, 119991 Moscow, Russia; e-mail: hkww@ran.gpi.ru, oficerov@ran.gpi.ru

Received 28 July 2010; revision received 13 January 2011
Kvantovaya Elektronika **41** (3) 239 – 242 (2011)
Translated by I.A. Ulitkin

2. System model

The scheme of the considered laser cavity + active mirror system is shown in Fig. 1. In modelling the system under study, we developed the operator model [6], which was proposed for the Fabr – Perot interferometer with nonflat mirrors and an adjustable gap. In this model, the eigenvalues γ and eigenfunctions U of the system are found from the equation

$$R_0 H_{\rm res} R_{\rm int} U = \gamma U, \tag{1}$$

where U is the field distribution at the output coupler; $R_0 = 1$ is reflection coefficient in the field amplitude for a mirror M0; $H_{\rm res}$ is the round-trip operator [8]; $R_{\rm int}$ is the reflectivity operator for the interferometer [6, 7]. Below we use the relations for the operators obtained to fit a system with infinitely thin nonabsorbing reflectors. The amplitude (in the field) reflectivities for mirrors M1, M2 are R_1, R_2, respectively. They are defined for the field inside the interferometer and considered independent of the coordinates of points on the reflector apertures. Transmission coefficients T_j ($j = 0, 1, 2$) are associated with R_j by the law of conservation of energy: $|R_j|^2 + |T_j|^2 = 1$. At the same time, the reflection and transmission coefficients for the field incident on the mirror M1 from the cavity have the form $-R_1^* \exp(\mathrm{i}\Psi)$ and $T_1^* \exp(\mathrm{i}\Psi)$, respectively [$\Psi$ is the phase additive (constant)] [9]. The aperture limitation and shape of the reflecting surface of each of the mirrors are

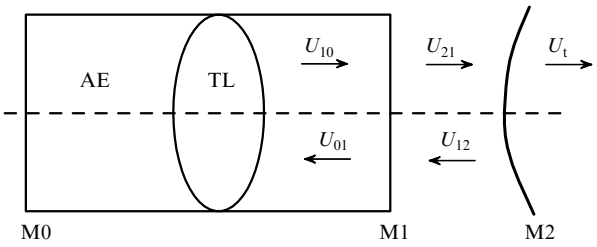

Figure 1. Scheme of the laser system with an active mirror: (AE) active element; (TL) thermal lens; (M0, M1) output and back cavity mirrors; (M2) output interferometer mirror; (U_t) the field distribution at the output of the laser system; (U_{01}, U_{10}, U_{12}, U_{21}) the field distributions in the plane of the aperture M1; (U_{01} and U_{10}) (U_{12} and U_{21}) the fields reflected from M1 and incident on it inside the laser cavity (inside the interferometer).

taken into account by the operators $M_j = A_j \exp(\mathrm{i}\alpha_j)$. Here, A_j is determined by the aperture of the jth mirror (within the aperture, $A_j = 1$; outside the aperture, $A_j = 0$); $\alpha_j = 2ks_j$; $k = 2\pi/\lambda$ is the wavenumber; λ is the radiation wavelength; s_j is the coefficient taking into account the deviation of the shape of a reflector from plane. Propagation of the field through a coupler reduces to multiplication of the field by the corresponding transmission coefficient. Propagation of radiation from the aperture plane of the nth mirror to the mth operator is described by the operator K_{mn}. Taking into account the above assumptions and notations

$$R_{\mathrm{int}} = \exp(\mathrm{i}\Psi)(-R_1^* A_1 E + R_2 H_{\mathrm{int}})(E - R_1 R_2 H_{\mathrm{int}})^{-1}, \quad (2)$$

where $H_{\mathrm{int}} = \sqrt{M_1} K_{12} M_2 K_{21} \sqrt{M_1}$ is the round-trip operator for the interferometer with allowance for reflections from mirrors M1 and M2, and E is the unit operator.

In equation (1) $H_{\mathrm{res}} = \sqrt{M_1^*} K_{10} M_0 K_{01} \sqrt{M_1^*}$. If we assume that the coefficient R_1 or R_2 is zero, which is equivalent to the absence of the interferometer in the system, equation (1) is transformed into an equation for the laser resonator.

The field entering (1) has the form

$$U = \sqrt{M_1^*} U_{10}, \quad (3)$$

and the field at the system output has the form

$$U_{\mathrm{t}} = T_2 A_2 K_{21} A_1 U_{21}. \quad (4)$$

Field distributions U_{01} and U_{21} are determined from the system of equations

$$\begin{aligned} U_{10} &= \exp(k_{\mathrm{a}}) K_{10} R_0 M_0 K_{01} A_1 U_{01}, \\ U_{12} &= K_{12} M_2 R_2 K_{21} A_1 U_{21}, \\ U_{01} &= T_1 A_1 U_{12} - \exp(\mathrm{i}\Psi) R_1^* M_1^* U_{10}, \\ U_{21} &= \exp(\mathrm{i}\Psi) T_1^* A_1 U_{10} + R_1 M_1 U_{12}. \end{aligned} \quad (5)$$

In the first equation there is the factor $\exp(k_{\mathrm{a}})$, where k_{a} is a complex gain, taking into account also the phase shift per round trip in the laser resonator.

Let us explain the physical meaning of equations (5). The first equation describes (with allowance for the gain) the round trip of radiation in the laser cavity, the second – the round trip of radiation in the interferometer-based mirror, the third – the formation of the field distribution with account for radiation entering the laser cavity from the interferometer, and the fourth – the formation of the field distribution in the interferometer with account for radiation emerging from the laser cavity. The solution of the system is easy to obtain via algebraic transformation with the substitution of $\exp(-k_{\mathrm{a}})$ by γ.

In view of system (5), the field (4) at the system output after passing through a coupler M2 is calculated as

$$U_{\mathrm{t}} = \exp(\mathrm{i}\Psi) T_1^* T_2 A_2 K_{21} \sqrt{M_1} (E - R_1 R_2 H_{\mathrm{int}})^{-1} U. \quad (6)$$

Equation (1) is valid in the geometric approximation as well as in the diffraction one. In general, the last operator-factor in formula (2) can be specified as a series expansion:

$$(E - R_1 R_2 H_{\mathrm{int}})^{-1} = \sum_{n=0}^{\infty} (R_1 R_2 H_{\mathrm{int}})^n.$$

This representation corresponds to summation of fields that are formed upon multiple reflections inside the interferometer-based mirror. If the field is described by the diffraction Fresnel – Kirchhoff integral, the field distribution of each of the following summed beams can be obtained by integration, on the basis of the field distribution in the previous beam: $(R_1 R_2 H_{\mathrm{int}})^{n+1} = (R_1 R_2 H_{\mathrm{int}})(R_1 R_2 H_{\mathrm{int}})^n$.

In this paper, we used in the calculations the matrix description of the operators associated with the replacement of integration (in the diffraction approximation) by discrete summation [6]. In this case, the operator $(E - R_1 R_2 H_{\mathrm{int}})^{-1}$ is defined as the inverse operator $(E - R_1 R_2 H_{\mathrm{int}})$.

The model makes it possible to optimise the characteristics of the resonator + interferometer-based mirror system, taking into account thermal lens and requirements imposed on the parameters of output radiation. Below we discuss the results of numerical studies of the microchip laser + active mirror system.

3. Results of numerical experiments

The results of calculations of the basic characteristics of the laser system considered in [7] are shown in Figs 2–4. The data in Figs 2, 3 refer to the strip geometry, and the data in Fig. 4 – to a cylindrically symmetric system (circular mirrors).

The initial resonator is made of flat mirrors M1 and M0, and the interferometer – of the output resonator mirror M1 and a spherical mirror M2. Below in accordance with the terminology used to describe the optical cavities, the interferometer is called stable or unstable.

Figure 2 shows the dependences of $|\gamma|^2$ on the mode number of the microchip laser. The thermal lens distributed along the length of the laser cavity was simulated by an

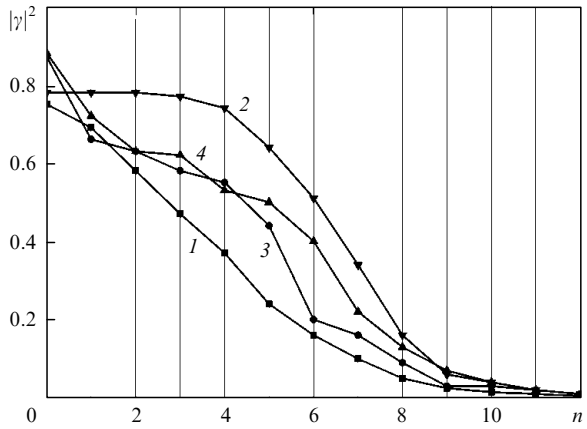

Figure 2. Dependences of $|\gamma|^2$ on the mode number n: plane-parallel resonator with thermal lens (*1*), resonator with thermal lens (*2*), resonator with a stable interferometer and thermal lens (*3*), resonator with an unstable interferometer and thermal lens (*4*).

infinitely thin lens located in the middle of the cavity. System parameters: the radius of curvature of the output mirror, ± 0.06 m; the wavelength, $\lambda = 1.064$ μm; the interferometer length, $l = l_0 + \Delta l$ ($l_0 = 100\lambda$, Δl is the interferometer detuning within $0 - \lambda/2$); the diameter of the output aperture of the cavity, $d = 20$ μm; reflectivities, $R_1 = R_2 = 0.8$; the focal length of the thermal lens, 6 mm; the cavity length, $l_r = 5.5$ mm; the refractive index of the active element, 1.82. It follows from the analysis of the numerical results and Fig. 2 that in the presence of thermal lens [curve (*2*)] the resonator becomes a multimode one. The radiation divergence was assessed from the data presented in Fig. 2, taking into account the number of modes [10] that fall in the region $|\gamma|^2 > |\gamma_s|^2$, where $|\gamma_s|^2 = 0.2 - 0.6$ is the threshold value, corresponding to an increase in radiation of the microchip Nd:YAG laser ($|\gamma_s|^2 = \exp(-k_a), k_a = 2l_r k_u$; the gain, $k_u = 0.5$–$1.5\ \mathrm{cm}^{-1}$). In this case, the divergence of the output radiation in the cavity with thermal lens is 2–2.5 times higher than the divergence of radiation in the resonator without thermal lens. With the interferometer as the output mirror [curves (*3, 4*)], the system operates in the close-to-single-mode regime.

The characteristics of the cavity + interferometer-based mirror system depend strongly on the controlled detuning of the interferometer Δl (Fig. 3). In Fig. 3, $|\gamma|^2$ is the square of the modulus of the eigenvalues for the dominant mode; $\Delta|\gamma|^2$ is the difference between the squares of the modulus of the eigenvalues for the dominant mode and the mode nearest to it; and the parameter ω is proportional to the divergence Θ of the output radiation in the far field at the 0.5 level (of the total power) for the dominant mode: $\Theta = 2\lambda\omega/(\pi d)$. The data in Fig. 3 refer to an unstable interferometer. In the region of detunings $(0.22 - 0.45)\lambda$, the TEM_0 mode is dominant, while in the region of detunings $(0.18 - 0.22)\lambda$, the TEM_1 becomes dominant. Breaks in the ω dependence (Fig. 3) are due to the change in the number of the dominant mode when changing the interferometer detuning. The value of $|\gamma|^2$ depends strongly on the interferometer detuning. Thus, $|\gamma|^2$ for the mode TEM_0 ranges from 0.58 to 0.9, which makes it possible to control the output power. The radiation divergence in this case does not change by more than 25 %.

Figure 4 shows the results of numerical studies of a practically important case of a system with a cylindrically symmetric geometry (circular mirrors) with a spherical or an aspherical reflector M2. To classify the modes of these systems, it is possible to use the notation TEM_{nm}, which is the same as for the modes [8] of the spherical laser resonators ($n, m = 0, 1, 2,...$ are the azimuthal and radial indices, respectively). In a system with a spherical interferometer $\Delta l = 0.32\lambda$, the radius of curvature of the output mirror of the interferometer is 0.02 m, other parameters are the same as those discussed above for the strip resonator. In the case of an aspherical interferometer $\Delta l = 0.49\lambda$ and shape of the reflector is given by a super-Gaussian function $s_2(\boldsymbol{r}) = (-\lambda/2)\exp[-(2r/a)^6]$ ($\boldsymbol{r}$ is the radius vector of a point in the plane of the aperture in the cylindrical coordinate system with the axis z, which coincides with the optical axis of the system).

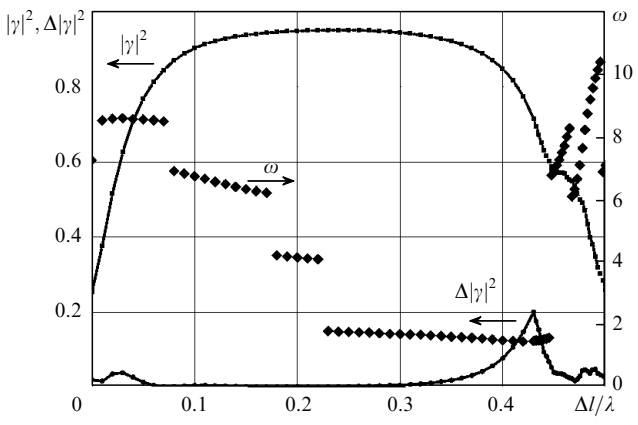

Figure 3. Dependences of $|\gamma|^2$, $\Delta|\gamma|^2$, and ω on the detuning $\Delta l/\lambda$.

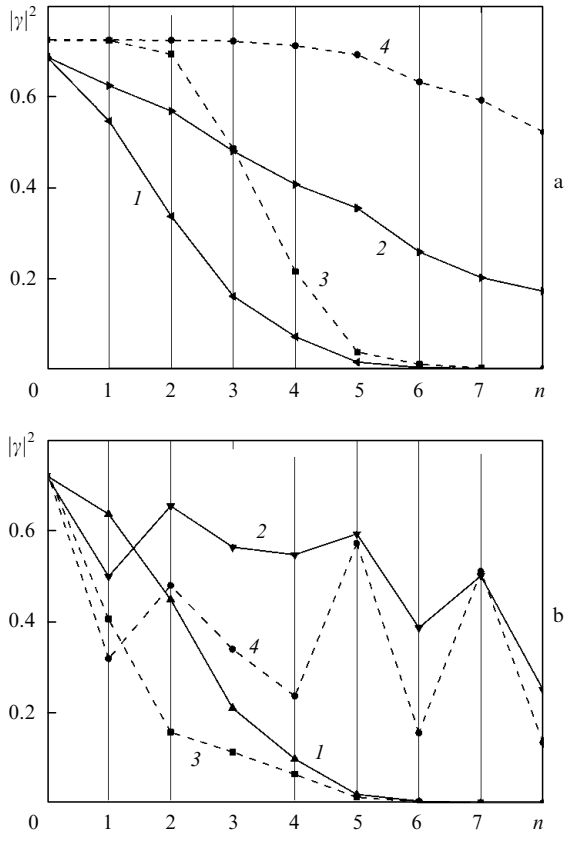

Figure 4. Dependences of $|\gamma|^2$ on the mode number n: reference plane-parallel resonator without thermal lens (*1, 2*), with thermal lens (*3, 4*) (a), resonator with the thermal lens + unstable spherical interferometer system (*1, 2*) and the resonator with thermal lens + aspherical interferometer system (*3, 4*) (b). Curves (*1, 3*) refer to TEM_{0n} modes; (*2, 4*) – to TEM_{n0} modes.

In the computing experiment performed the account for thermal lens leads to an increase in the radiation divergence of the reference plane-parallel resonator by 4–6 times. The use of a spherical interferometer-based mirror in the cavity is accompanied by a decrease in the divergence by a factor of 1.5–2.5. In this case, the detuning Δl, where TEM_{00} is the dominant mode, is equal to $(0.28 - 0.38)\lambda$. The comparative analysis of curves (*1, 2*) (Fig. 4a) and (*3, 4*) (Fig. 4b) shows that the use of an aspherical interferometer-based mirror brings the radiation divergence nearer to the divergence of radiation in a system without thermal lens. The effect of the active mirror on the system selectivity is more pronounced

with respect to the radial index (Fig. 4). The lower azimuthal-index selectivity results from the cylindrically symmetric interferometer-based mirror. In comparison with a strip resonator, the system with circular mirrors (with comparable technical parameters) is characterised by a 1.5–2 times greater divergence, which is consistent with the results of [10] for spherical cavities.

It should be noted that the purpose of the performed investigations of the laser system with an aspherical reflector is the estimate of the potential effectiveness of its application. At the optimal selection of the parameters, the aspheric interferometer is used as the output reflector of the laser cavity, provides lower power losses and smaller divergence of the output radiation in comparison with the system with a spherical interferometer. Using an active deformable (adaptive) mirror as an aspherical reflector greatly enhances the system potential in terms of the formation of the distribution function of the reflectivity by changing the shape of the active reflector. As an active deformable mirror use can be made of reflectors [11] with a bending moment. An important advantage of the system under study is the feasibility to control the reflectivity of the active mirror with a frequency of $\sim$100 Hz or higher.

Based on the results, it seems appropriate to study in more detailed the efficiency of application of an interferometer-based mirror with aspheric or deformable reflectors with account for real limitations on shaping. In this case, the search for the optimal shape of the reflecting mirror surface can be based, inter alia, on the methods of inverse optical problems.

4. Conclusions

The numerical study of a microchip laser with thermal lens showed that the use of an active output cavity mirror based on a Fabry–Perot interferometer allows one to control the mode composition and divergence of output laser radiation. At the optimum detuning and radii of curvature of the interferometer mirrors the radiation divergence can be reduced by 1.5–2.5 times. A promising way to improve the system performance and capacity is associated with the use of an aspherical (or active, adaptive) mirror in the interferometer-based mirror or laser cavity.

Acknowledgements. This work was supported by the Russian Foundation for Basic Research (Grant No. 09-02-00343).

References

1. Molva E. *Opt. Mater.*, **11**, 289 (1999).
2. Zayhowski J.J. *Laser Focus World*, **32** (4), 73 (1996).
3. Kiiko V.V., Ofitserov E.N. *Kvantovaya Elektron.*, **36** (5), 483 (2006) [*Quantum Electron.*, **36** (5), 483 (2006)].
4. Kravtsov N.V., Nanii O.E. *Kvantovaya Elektron.*, **20** (4), 322 (1993) [*Quantum Electron.*, **23** (4), 272 (1993)].
5. De Silvestri S., Laporta P., Magni V., Svelto O. *Opt. Lett.*, **12**, 84 (1987).
6. Kiiko V.V., Kislov V.I., Ofitserov E.N. *Kvantovaya Elektron.*, **40** (6), 556 (2010) [*Quantum Electron.*, **40** (6), 556 (2010)].
7. Kiyko V.V., Kislov V.I., Ofitserov E.N. *Techn. Progr. 14th Intern. Conf. on Laser Optics 'Laser Optics-2010'* (St. Petersburg, 2010) ThR4-p08, p. 72.
8. Anan'ev Yu.A. *Opticheskie resonatory i lasernye puchki* (Optical Resonators and Laser Beams) (Moscow: Nauka, 1990).
9. Troitskii Yu.V. *Mnogoluchevye interferometry otrazhennogo sveta* (Multibeam Reflected-Light Interferometers) (Novosibirsk: Nauka, 1985).
10. Golyaev Yu.D., Zverev G.M. *Lazery na kristallakh i ikh primenenie* (Crystal Lasers and Their Applications) (Moscow: Radio i Svyaz', 1986).
11. Taranenko V.G., Shanin O.I. *Adaptivnaya optika v priborakh i ustroistvakh* (Adaptive Optics in Instruments and Devices) (Moscow: FGUP 'TsNIIAtominform', 2005).